Applied Physics A (2020) 126:475
https://doi.org/10.1007/s00339-020-03650-y

Applied Physics A
Materials Science & Processing

Growth dynamics of pulsed laser deposited WS_2 thin films on different substrates

Gobinda Pradhan[1] · Partha P. Dey[1] · Ashwini K. Sharma[1]

Received: 13 January 2020 / Accepted: 18 May 2020 / Published online: 1 June 2020

Abstract
The scaling behavior, as well as growth mechanism of polycrystalline WS_2 thin films grown on glass and Si substrates by pulsed laser deposition as a function of the deposition time, has been studied using height–height correlation function using the AFM images. X-ray diffraction measurement confirms the increase in crystallinity of the WS_2 thin film on both the substrates. The WS_2 films deposited onto Si substrate showed high rate of roughening or interface width (w) and a rapid increase in island size or correlation length (ξ) of WS_2 nanoclusters in comparison to the films deposited onto glass substrate. The WS_2 films grown on glass substrate evolved following the nonlinear stochastic deposition equation, however, WS_2 films on Si substrate follow a linear growth model. The difference in surface smoothness, thermal conductivity and sticking coefficient of the two substrates causes different growth patterns of WS_2 films onto the substrates. The growth of the WS_2 films on the two different substrates evolved differently which has been realized more conveniently by schematically analyzing the behavior of the evolution of ξ and w with deposition time, t. The high roughness of the films deposited onto oxidized Si provides a large surface area, which will be useful for electro-catalysis applications.

Keywords WS_2 thin films · Pulsed laser deposition · Growth dynamics · Height-height correlation function

1 Introduction

Layered transition metal dichalcogenide (TMDC) materials have emerged as a class of two-dimensional (2D) materials with excellent electronic and optical properties [1–3]. Among them, WS_2 has drawn tremendous attention due to its attractive properties like thickness dependent bandgap of 1.2 (indirect) to 1.9 (direct) eV, high electron mobility, high electronic on–off switching ratio, efficient photo responsibility, etc. [4–6]. In the last few years, pulsed laser deposited monolayer to multilayered as well as bulk-like WS_2 films demonstrated their efficient uses as photodetector, catalyst and other advanced electronics and optoelectronic devices [7–9]. Surface morphology of a thin film does regulate many of the physical and chemical properties which have a sharp impact on the device performance of the respective films. The growth dynamics of thin films represented by scaling theory is a useful tool to explain the evolution of the surface morphology of thin films and to formulate theoretical models of growth modes for different organic and inorganic materials [10–13]. So the understanding of the growth dynamics of the deposited thin films is important to develop an optimized thin film for efficient device performance. However, despite the rapid progress in applications of WS_2 layered films, there is no such report on scaling behavior and growth dynamics of WS_2 films. Hence, we undertake a comparative study on the growth evolution of a few layered to bulk-like WS_2 films on two different substrates, in the light of scaling theory and stochastic growth equation. Height-height correlation function (HHCF) is fitted with an appropriate theoretical model to evaluate the interface width (w) and lateral correlation length (ξ) of the films of various deposition time. The surface morphology properties of the films measured and presented statistically in terms of various scaling exponents like short range (local) as well as long-range (global) roughness exponents (α_{loc} and α), growth exponent (β), dynamic scaling exponent ($1/z$), etc. Further, the growth mechanism of the WS_2 films are compared with the linear and nonlinear stochastic thin film growth equations. This understanding can enable one to attain controlled growth of a film required

✉ Ashwini K. Sharma
aksharma@iitg.ac.in

[1] Department of Physics, Indian Institute of Technology Guwahati, Guwahati, Assam 781039, India

in different catalytic, photo harvesting and field emission applications [14, 15].

2 Experimental methods

WS_2 thin films were deposited onto Corning glass and oxidized Si (SiO_2/Si-300 nm/380 µm) substrate via pulsed laser deposition (PLD) by focusing a 2rd harmonic, Q-switched Nd:YAG laser (Quanta-Ray INDI, $\lambda = 532$ nm, pulse duration—8 ns and repetition rate—10 Hz) on polycrystalline WS_2 target (pellet), at a laser fluence of ~ 2.2 J/cm^2 under vacuum (~ 5×10^{-6} mbar). The films were deposited for various deposition times of 30 s, 2, 5, 10, 15 and 20 min duration at a substrate temperature of 400 °C. During the deposition the target to substrate distance was maintained at 5 cm. Crystalline structure of the films was characterized by X-ray diffractometer (Rigaku TTRAX III). Cu K_α line was used as X-ray source and the measurements were carried out at a glancing incidence angle of $\omega = 1°$. The scanning was performed at an angular step of 0.03°. AFM (Bruker- Innova) was operated in the non-contact mode to study the layered structure, morphology, dynamic scaling and growth mechanism of WS_2 films. All the AFM images were recorded with the same scanned speed where 2-micron size images were recorded by 512 number of line scan.

3 Results and discussion

Figure 1a, b shows the XRD pattern of WS_2 films grown on Corning glass and oxidized Si substrate, respectively. There is no significant XRD signal in the WS_2 films on glass substrate up to deposition time of 5 min and thereafter prominent XRD peaks correspond to WS_2 (002), (101) and (103) crystalline plane were observed [7, 16, 17]. The XRD pattern of the films confirmed an increase in crystallinity with the deposition time. The XRD pattern of WS_2 films deposited on oxidized Si from 30 s to 10 min showed a sharp peak corresponding to WS_2 (006) crystalline plane while with an increase in deposition time, XRD peaks corresponding to WS_2 (002), (101), (103) planes started appearing after 10 min [7, 16, 17]. The deposited WS_2 films exhibit polycrystalline nature irrespective of deposition time and underlying substrates. The crystallite sizes of the WS_2 films are measured by using the Debye Sherrer formula, defined as, $D = \frac{0.89\lambda}{\beta \mathrm{Cos}\theta}$, where D is the average crystallite size and λ is the X-ray wavelength ($\lambda = 1.5406$ Å). β and θ are the full width at half maxima (FWHM) of XRD peak and the diffraction angle of the corresponding XRD peak. The most intense peak corresponding to (101) plane for WS_2 films onto glass substrate and (006) plane for WS_2 films onto SiO_2/Si substrate were considered to measure the crystallite size of the respective films. The average crystallite size of the WS_2 films on glass substrate at deposition time of 10, 15 and 20 min were 10.7, 12.3 and 9.1 nm, respectively, while the crystallite size of the WS_2 films on SiO_2/Si at deposition time of 30 s, 2, 5, 10, 15, and 20 min were estimated to be 44.7, 42.5, 51.5, 44.7, 50 and 51.5 nm, respectively, which suggest WS_2 films deposited onto SiO_2/Si substrate are more crystalline than the films deposited onto glass substrate. Using surface profilometer, the thicknesses of the films deposited onto glass substrate for 5, 10, 15 and 20 min deposition time are estimated to be 23.8, 44.2, 68.0 and 85.3 nm, respectively, while films onto SiO_2/Si substrate showed

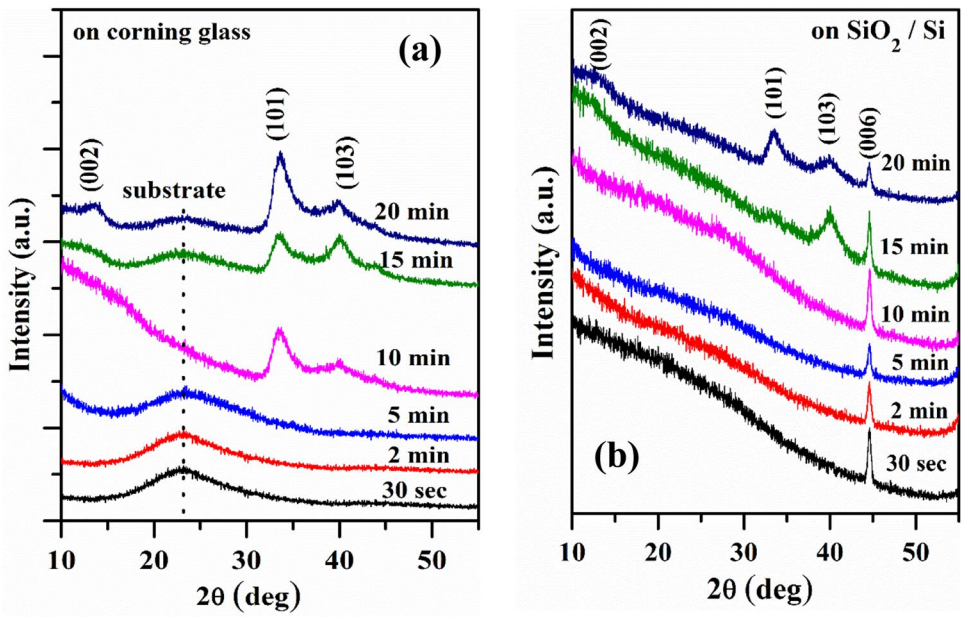

Fig. 1 XRD pattern of WS_2 films on **a** corning glass and **b** oxidized Si substrate for different deposition times (30 s–20 min) [JCPDS Card No: 08-0237]

thicknesses of 26.0, 48.6, 71.3 and 89.2 nm for the deposition time 5, 10, 15 and 20 min, respectively. Film deposited at 2 min and 30 s could not be measured accurately due to much lower thickness.

The surface morphology and growth dynamics of the films were characterized systematically using AFM images. Figure 2a and 3a shows the AFM images (2 μm×2 μm) of WS_2 films grown onto the Corning glass and oxidized Si substrate at 400 °C substrate temperature with 30 s, 2, 5, 10, 15 and 20 min deposition time, respectively. The scaling exponents (α_{loc}, β, $1/z$) have been estimated from HHCF, $H(r,t)$, to understand the growth processes and the dynamic scaling behavior involved during PLD of WS_2 films. $H(r,t)$ is defined as statistical average of the mean square of height difference between two positions on the surface separated by an in-plane distance r $(=\sqrt{(x-x')^2+(y-y')^2})$, as $H(r,t) = \left|h(r+r',t)-h(r',t)\right|^2$, where $h(r+r',t)$ and $h(r',t)$ are the heights of the film surface at the positions of (x, y) and (x', y'). HHCF is usually extracted from AFM images by spatial averaging over a region where the size of the region should be much larger than r to avoid edge effects. Based on the relative magnitudes of r and ξ; HHCF shows two different characters, (1) for $r << \xi$, $H(r,t) \sim [m(t)r]^{2\alpha_{loc}}$, where $m(t)$ is the local slope and α_{loc} is the local roughness exponent, which corresponds to short-range roughness of a self-affine surface, and (2) for $r \gg \xi$, $H(r,t) \sim 2w^2$, where $w = \sqrt{([h(r,t)]^2)}$ is the interface width or RMS roughness. w can be expressed by a simple dynamic scaling called as Family–Vicsek relation, $w = t^{\beta} f\left(\frac{r}{t^{\beta/\alpha_{loc}}}\right)$ where $f\left(\frac{r}{t^{\beta/\alpha_{loc}}}\right) \sim \begin{cases} \text{contant} & \text{where, } r \gg t^{\beta/\alpha_{loc}} \\ \left(\frac{r}{t^{\beta/\alpha_{loc}}}\right)^{\alpha_{loc}} & \text{and} \\ \left(\frac{r}{t^{\beta/\alpha_{loc}}}\right)^{\alpha_{loc}} & r \ll t^{\beta/\alpha_{loc}} \end{cases}$ and $r \le L$ (L is system size) while α_{loc} and β are the local roughness and growth exponents, respectively [18, 19]. From the above relation it is observed that for small r (i.e. $r \ll t^{\beta/\alpha_{loc}}$), w become independent of deposition time, t and relate as $r^{\alpha_{loc}}$, but for large r, β become independent of r and scale as the power law, $w \sim t^{\beta}$. These two behaviors crossover at $r = \xi$, the lateral correlation length within which surface heights are significantly correlated. The HHCF used to fit with appropriate theoretical model to determine the interface width (w) and lateral correlation length (ξ) as they evolve with deposition time, t. For dynamic scaling, the growth parameters w and ξ are dependent on the deposition time (t), and varies with t as $w \sim t^{\beta}$ and $\xi \sim t^{1/z}$ [20, 21] where β is

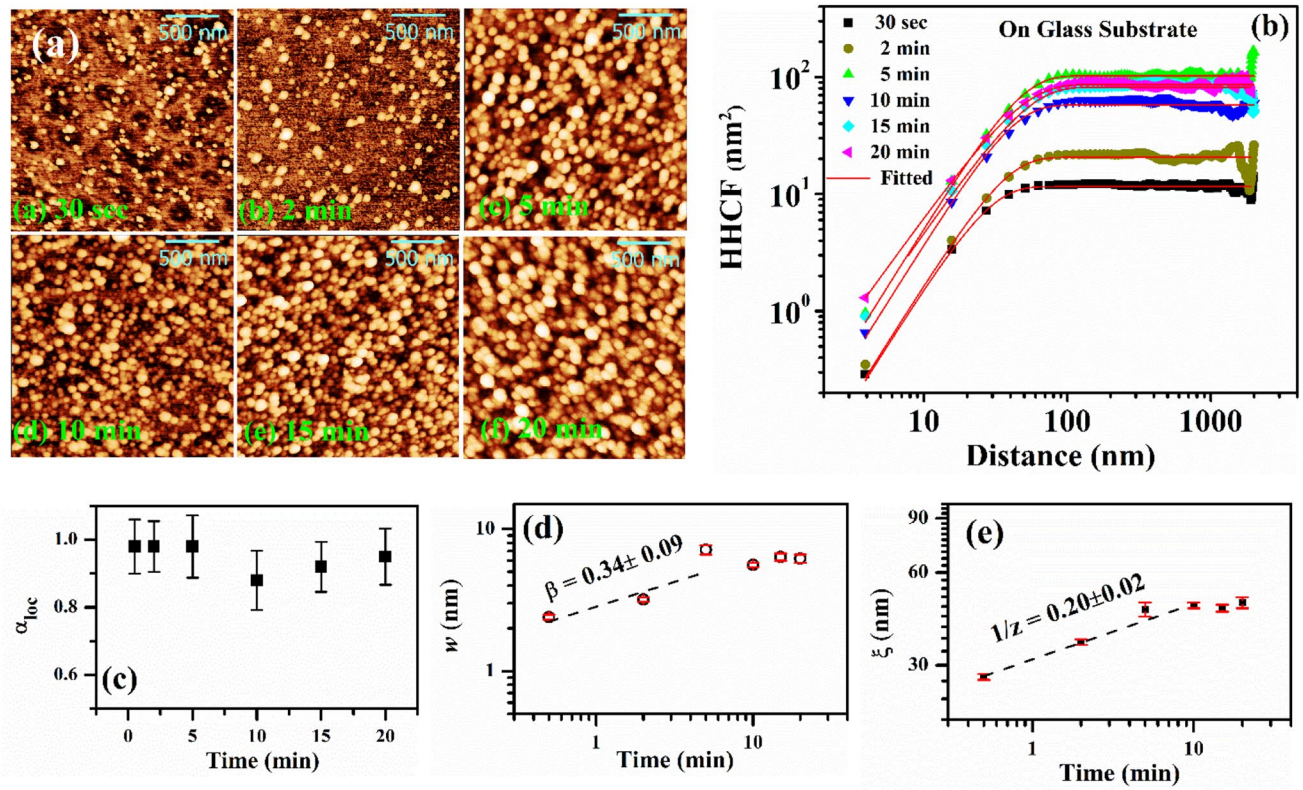

Fig. 2 **a** AFM images of 2×2 μm scanned area of the top surface of PLD WS_2 films on Corning glass for different deposition times 30 s, 2, 5, 10, 15 and 20 min. **b** Log–Log plot of HHCF, $H(r)$ as a function of distance r with best fitted theoretical curve for WS_2 thin films on Corning glass substrate with different deposition times. The symbols are experimental data and the red solid lines are fitted with Eq. (1). Plot of **c** surface roughness w, **d** correlation length ξ, and **e** roughness exponent α_{loc} as a function of deposition time, t

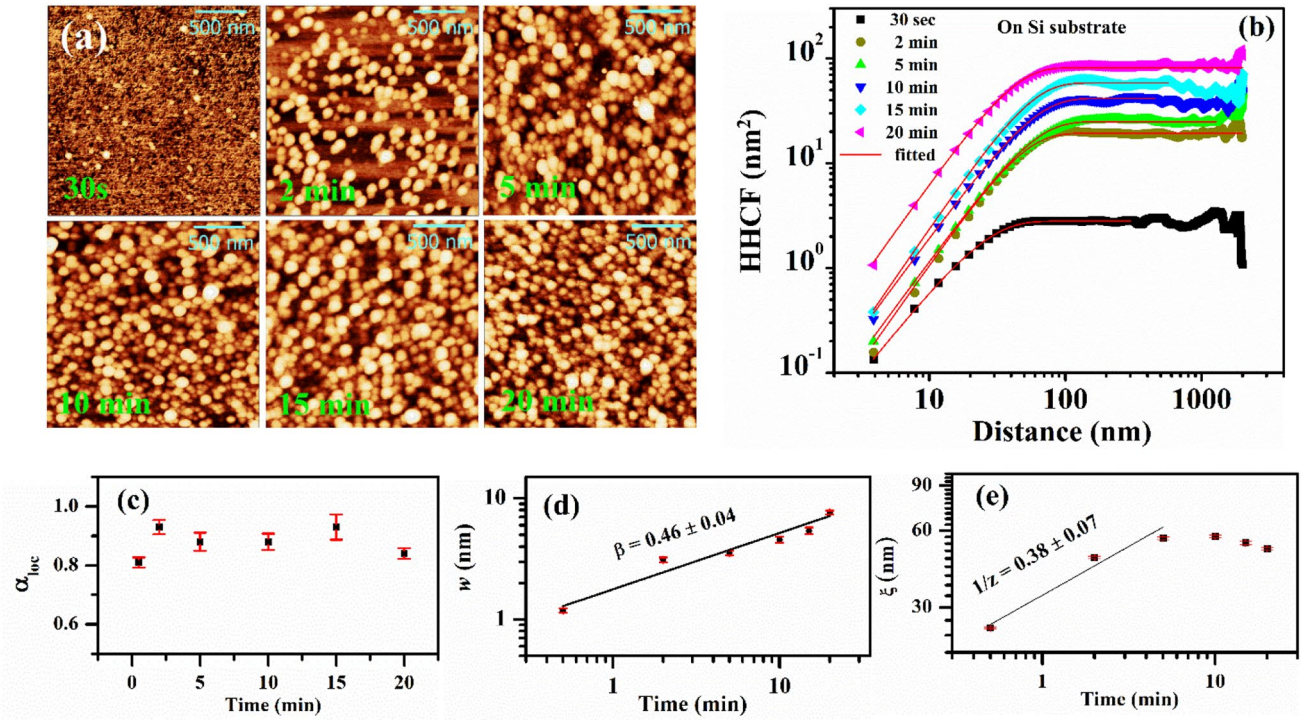

Fig. 3 **a** AFM images of 2 × 2 μm scanned area of the top surface of PLD WS_2 films on oxidized Si substrate for different deposition times 30 s, 2, 5, 10, 15 and 20 min. **b** Log–Log plot of HHCF, $H(r)$ as a function of distance r with best fitted theoretical curve for WS_2 thin films on oxidized Si substrate with different deposition times. The symbols are experimental data and the red solid lines are fitted with Eq. (1). Plot of **c** surface roughness w, **d** correlation length ξ, and **e** roughness exponent α_{loc} as a function of deposition time, t

growth exponent while $1/z$ is termed as the dynamic scaling exponent. Here, β signifies the pace of surface roughening while $1/z$ represents the rate of lateral growth of correlated structure (islands). The specific set of exponents α_{loc}, β and $1/z$, follow a specific theoretical model, which presents a particular growth mechanism that governs the evolution of surface are said to form a universality class. The set of exponents α_{loc}, β and $1/z$, corresponds to a specific universality class and their value does suggest the underlying mechanism that governs the evolution of the surface. The HHCF is represented by exponential correlation model, as [20],

$$H(r) = 2w^2\left[1 - \exp\left[-\left(\frac{r}{\xi}\right)^{2\alpha}\right]\right] \quad (1)$$

From Figs. 2b and 3b, it is observed that HHCF, $H(r, t)$ corresponding to the WS_2 films on glass and oxidized Si substrate increased linearly with r at small r and saturates at large r, with the asymptotic behavior predicted by Eq. (1) [20]. It is clear from Fig. 2b that $H(r, t)$ shifted upward as film thickness increased with growth time up to 5 min then they almost overlapped with each other for further deposition time, which confirmed that the RMS roughness increased initially as the films grew and then got saturated after deposition time of 5 min. Figure 3b shows a systematic increment in $H(r, t)$ with increasing growth time suggesting the roughening of the films with the deposition time. The HHCF curves were fitted using Eq. (1), to estimate α_{loc}, $w(t)$ and $\xi(t)$. The variation of these parameters with deposition time was studied to understand the growth dynamics. α_{loc} is the short-range or local surface roughness coefficient of a film where the position difference of two points (r) on the surface is much less than the correlation length (ξ) of the film.

Figures 2c and 3c show the variation of α_{loc} with deposition time. The average value of α_{loc} for the films deposited onto Corning glass and oxidized Si are ~ 0.93 ± 0.08 and ~ 0.88 ± 0.02, respectively. In general, α_{loc} lies between 0 to 1, where, a smaller value of α_{loc} corresponds to the more locally rough surface while the larger α_{loc} of the present films corresponds to locally smooth surface. Therefore, the observed value of α_{loc} suggests that WS_2 films deposited onto Corning glass were smoother than the top surface of the WS_2 films deposited onto oxidized Si. Figures 2d and 3d show Log–Log variations of w versus time (t) for the films deposited onto Corning glass and oxidized Si. In the case of WS_2 films on corning glass, the RMS roughness (w) increased linearly up to 5 min and then saturated beyond it while WS_2 films on Si showed a continuous increment in w

with deposition time. The growth exponent (β) corresponding to the WS_2 films on glass and Si are 0.34 ± 0.09 and 0.46 ± 0.04. The larger β value of WS_2 films on Si substrate suggested high rate of roughening of WS_2 films surface during growth on Si substrate.

Figures 2e and 3e show ξ versus t plot in log scale. In case of both the substrates, the value of ξ increased as $\xi \sim t^{1/z}$ initially from 30 s to 5 min but beyond this ξ saturated. The values of $1/z$ extracted from ξ versus t plot are 0.20 ± 0.02 and $\sim 0.38 \pm 0.07$ corresponding to WS_2 films on Corning glass and Si substrate, respectively. A higher value of $1/z$ of WS_2 films on Si suggested a rapid increase in island size of WS_2 nanoclusters onto Si substrate. The large β and $1/z$ of the WS_2 films deposited onto Si compared to WS_2 films deposited onto Corning glass suggested high roughening as well as large size WS_2 nanoclusters islands formation onto Si substrate at the same deposition time. This can be attributed to comparatively high thermal conductivity and smoothness of surface of Si substrate which caused more diffusion of the adatoms to form the large size clusters in Si substrate. Hence, the WS_2 films deposited onto Corning glass grew in both vertical and lateral dimensions up to deposition time of 5 min and then saturated while the lateral growth of WS_2 films on Si substrate got fixed after 5 min deposition time but vertical growth continuously increased with the deposition time.

Under dynamic scaling, $\alpha_{loc} = \beta z$ but in the present study on both the substrates, dynamic scaling failed ($\alpha_{loc} \neq \beta z$) which implies the height profile may follow another scaling hypothesis called anomalous scaling where the global (α, β) and local (α_{loc}, β_{loc}) exponents are different from each other. In case of long-range or global roughness exponent (α), the position difference of two points (r) on the surface is much larger than the correlation length (ξ) of the film. The global roughness exponents α ($\sim \beta z$) are 1.75 and 1.21 in the case of glass and Si substrate, which are different from α_{loc}. The observed $\alpha > 1$ suggests a high surface roughening of the WS_2 films.

The difference in surface evolution of WS_2 film on the two different substrates can be realized more conveniently by schematically analyzing the behavior of the evolution of ξ and w with t as presented in Fig. 4a, b. At the initial stage of growth (30 s) sparsely distribution of nucleated WS_2 nanoclusters were observed on both the substrates. The surface coverage of the substrate by nucleated WS_2 was less at this stage. Nucleation continued until the surface was fully covered by a maximum number of highly dense nuclei. With further deposition, the impinging adatoms were captured by the nuclei and transformed into small size cluster. After that, around the deposition time of 2 min, a second different growth stage was observed where both ξ and w were larger than the initial stage. This means that with increasing deposition time the WS_2 clusters grew both in lateral and vertical directions. The observation suggests that all the impinging atoms were captured by the pre-deposited WS_2 clusters and only a few new nuclei formed. The typical vertical and lateral growth proceed by adsorption of fresh adatoms and diffusion of pre-deposited adatoms, and the film thickness, as well as surface coverage, increased rapidly. A further increase in the growth of ξ occurred at deposition time of 5 min. This growth stage was characterized by a coalescence of the WS_2 clusters leading to large sized clusters formation. At this stage, the cluster mobility was high and they moved along the surface and approached other clusters and led to a permanent diffusion-driven coalescence. Finally, after fully covering the substrate surface area by WS_2 clusters, lateral growth ceased while adsorptive growth progressed only in the vertical direction. During the vertical growth it was observed that while w further increased for WS_2 films on Si substrate, it saturated in case of WS_2 films on glass substrate [22]. The saturation of surface roughness

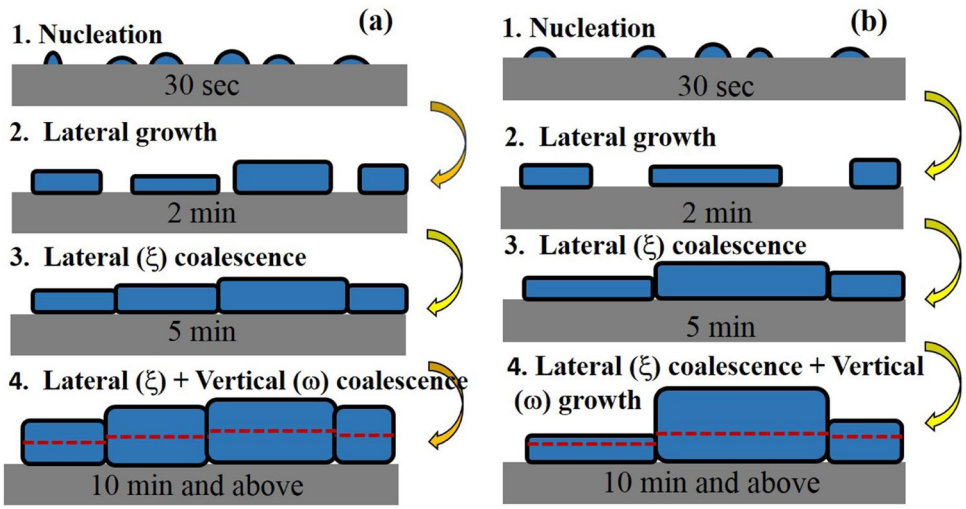

Fig. 4 Schematic picture of the growth evolution of the WS_2 films as a function of deposition time (t) deposited onto **a** corning glass and **b** oxidized Si substrate

(w) in the case of glass substrate at higher deposition time can be realized as follows. On the glass substrate, the underlying clusters (ξ) are of small sizes, as a result the freshly arrived adatoms onto the WS_2 film surface can easily equilibrate with the previous surface structure by only a small amount of particle diffusion which causes almost no change in surface roughness with further increase in deposition time above 5 min.

The growth mode and the dynamics of surface morphology of thin films can be expressed in linear and nonlinear stochastic partial differential equations. The gradients of the surface profile $h(x, t)$ for linear growth and nonlinear growth are expressed as [23],

$$\frac{\partial h}{\partial t} = a_1\nabla^2 h + a_2\nabla^4 h + \eta \tag{2}$$

$$\frac{\partial h}{\partial t} = a_1\nabla^2 h + a_2\nabla^4 h + a_3\nabla^2(\nabla h)^2 + a_4(\nabla h)^2 + \eta \tag{3}$$

where a_1, a_2, a_3 and a_4 are the material dependent scalar coefficients and η represents the deposition noise that exists during growth. In Eq. (3), the first term on the right hand side corresponds to the deflection of the perpendicularly incident adatoms due to the interatomic forces between the pre-deposited surface atoms and the incident adatoms. The second and the third term on the right hand side of Eq. (3) are associated with the microscopic mechanisms of the surface diffusion of adatoms and the equilibration of the inhomogeneous concentration of the diffusing adatoms on the surface. The fourth term on the right hand side of Eq. (3) is the Kardar Parisi-Zhang (KPZ) form which corresponds to the additional volume increase caused by oblique particle incidence [24]. Films growth following Eq. (2) shows an initial increment in correlation length (ξ) with growth time (t) then saturates at higher deposition time whereas the surface roughness (w) of the films continue to increase with the deposition time (t) [23]. On the other hand, film growth according to Eq. (3) shows an initial increment in correlation length (ξ) and surface roughness (w) with growth time (t) then both the parameters saturates at higher deposition time [23]. Hence in the present study growth of WS_2 films onto glass substrate follow a nonlinear growth model (Eq. 3) while WS_2 films onto Si substrate follows the linear growth model (Eq. 2). The smoother surface, higher thermal conductivity causes high surface diffusion of the WS_2 adatoms onto the Si substrate surface. The higher sticking coefficient of Si substrate compared to the glass substrate causes rapid growth of WS_2 films onto Si substrate and results in linear growth of the film.

Different local models like Mullins diffusion model [25], Edwards-Wilkinson model [26] and KPZ model [24] provide $\beta = 0.25$,0 and 0.24, $\alpha_{loc} = 1$,0 and 0.38 while $z = 4$, 2 and 1.58, respectively, for 2 + 1 dimensions which do not match with the values of β, α and z observed in the present case. Thus, none of the local models depicting different Universality classes can exactly explain the type of growth observed here. The growth parameters of MoS_2, another TMDC 2D material, films deposited by PLD technique at almost similar deposition conditions were $\beta = 0.85 \pm 0.11$, $1/z = 0.49 \pm 0.09$, $\alpha_{loc} = 0.89 \pm 0.01$, and $\alpha = 1.72 \pm 0.1$. The growth of MoS_2 thin films also did not follow dynamics scaling ($\alpha_{loc} = \beta z$) but rather showed intrinsic anomalous scaling behavior [21]. The large value of β and $1/z$ of the MoS_2 films suggest high rate of surface roughening and lateral growth of the films with deposition time in comparison to the WS_2 thin films. The value of growth exponentials (α, α_{loc}, β, and $1/z$) previously reported by Neeti et al., Dolbec et al. and Auger et al. in PLD and sputtered deposited metallic and semiconductor films are close to the present work [27–29]. As PLD process is directional, (flux distribution ~ $\cos^p\theta$) substrate receives incoming species at wide distribution of angle varying from 0° to nearly $\theta_{1/2}$ ($=\cos^{-1}(1/2)^p$) [30]. $\theta_{1/2}$ is the angle between target surface normal and flux direction where flux density becomes half of maximum in vacuum and p (varies from 8 to 20) is the parameter decided by laser spot size, laser fluence and degree of ionization of plasma. Hence, the growth process occurs overwhelmingly under shadowing mechanism and angle-dependent variable particle flux density. These deposition conditions promoting nonlocal effects [31] like large shadowing for surface growth as observed in the PLD WS_2 films. Overall, the pulsed laser deposited thin films showed an increase in surface roughness with an increase in deposition time. The high roughness of the films deposited onto oxidized Si provides large surface area, which is useful for various applications like photodetector, charge storage device, electro-catalyst, etc. [32–35].

4 Conclusion

In conclusion, a comparative study on the growth evolution of WS_2 films with deposition time on glass and Si substrates was performed in the light of scaling theory and stochastic growth equation. The characteristic growth exponents (α_{loc}, β and $1/z$) were determined using HHCF, obtained from AFM images. The cluster size and RMS roughness of the WS_2 films on the two different substrates evolved differently with deposition time. The WS_2 films deposited onto Si substrate showed a rapid increase in size of WS_2 nanoclusters and higher surface roughening in comparison to the films deposited onto glass substrate. WS_2 films deposited onto glass substrate follow the nonlinear growth model while WS_2 films onto Si substrate follow the linear growth model.

The growth exponents estimated in the present case cannot be exactly related to any known universality classes based on both local and non-local growth models, suggesting that a different universality class needed to be defined. Various non-local effects like shadowing, angle-dependent variable particle flux density plays an important role in the evolution of growth of these PLD thin films.

Acknowledgements The authors acknowledged department of Physics, IIT Guwahati for XRD facility, Center for excellence in Nanoelectronics & Theranostic Devices, IIT Guwahati for AFM facility. The authors gratefully acknowledge Mr. Ankur Pandey for his kind help in AFM data recording.

References

1. X. Song, J. Hu, H. Zeng, Two-dimensional semiconductors: recent progress and future perspectives. J Mater. Chem. C **1**, 2952 (2013)
2. Q.H. Wang, K. Kalantar-Zadeh, A. Kis, J.N. Coleman, M.S. Strano, Electronics and optoelectronics of two-dimensional transition metal dichalcogenides. Nat. Nanotechnol. **7**, 699 (2012)
3. M. Xu, T. Liang, M. Shi, H. Chen, Graphene-like two-dimensional materials. Chem. Rev. **113**, 3766 (2013)
4. A.L. Elías, N. Perea-López, A. Castro-Beltrán, A. Berkdemir, R. Lv, S. Feng, A.D. Long, T. Hayashi, Y.A. Kim, M. Endo, Controlled synthesis and transfer of large-area WS2 sheets: from single layer to few layers. ACS Nano **7**, 5235 (2013)
5. X. Liu, J. Hu, C. Yue, N. Della Fera, Y. Ling, Z. Mao, J. Wei, High performance field-effect transistor based on multilayer tungsten disulfide. ACS Nano **8**, 10396 (2014)
6. M.W. Iqbal, M.Z. Iqbal, M.F. Khan, M.A. Shehzad, Y. Seo, J.H. Park, C. Hwang, J. Eom, High-mobility and air-stable single-layer WS_2 field-effect transistors sandwiched between chemical vapor deposition-grown hexagonal BN films. Sci. Rep. **5**, 10699 (2015)
7. T.A. Loh, D.H. Chua, A.T. Wee, One-step synthesis of few-layer WS 2 by pulsed laser deposition. Sci. Rep. **5**, 18116 (2015)
8. J. Yao, Z. Zheng, J. Shao, G. Yang, Stable, highly-responsive and broadband photodetection based on large-area multilayered WS_2 films grown by pulsed-laser deposition. Nanoscale **7**, 14974 (2015)
9. M. Schenato, C.L.A. Ricardo, P. Scardi, R. Edla, A. Miotello, M. Orlandi, R. Morrish, Effect of annealing and nanostructuring on pulsed laser deposited WS_2 for HER catalysis. Appl. Catal. A Gen. **510**, 156 (2016)
10. J. Jeffries, J.-K. Zuo, M. Craig, Instability of kinetic roughening in sputter-deposition growth of Pt on glass. Phys. Rev. Lett. **76**, 4931 (1996)
11. M. Pelliccione, T. Karabacak, C. Gaire, G.-C. Wang, T.-M. Lu, Mound formation in surface growth under shadowing. Phys. Rev. B **74**, 125420 (2006)
12. P.P. Chatraphorn, Z. Toroczkai, S.D. Sarma, Epitaxial mounding in limited-mobility models of surface growth. Phys. Rev. B **64**, 205407 (2001)
13. Y.-P. Zhao, J. Fortin, G. Bonvallet, G.-C. Wang, T.-M. Lu, Kinetic roughening in polymer film growth by vapor deposition. Phys. Rev. Lett. **85**, 3229 (2000)
14. K.H. Hu, X.G. Hu, X.J. Sun, Morphological effect of MoS2 nanoparticles on catalytic oxidation and vacuum lubrication. Appl. Surf. Sci. **256**, 2517 (2010)
15. D.J. Late, P.A. Shaikh, R. Khare, R.V. Kashid, M. Chaudhary, M.A. More, S.B. Ogale, Pulsed laser-deposited MoS_2 thin films on W and Si: field emission and photoresponse studies. ACS Appl. Mater. Interfaces. **6**, 15881 (2014)
16. J. Zabinski, M. Donley, S. Prasad, N. McDevitt, Synthesis and characterization of tungsten disulphide films grown by pulsed-laser deposition. J. Mater. Sci. **29**, 4834 (1994)
17. G. Pradhan, A.K. Sharma, Linear and nonlinear optical response of sulfur-deficient nanocrystallite WS_2 thin films. J. Mater. Sci. **54**, 14809 (2019)
18. J.J. Ramasco, J.M. López, M.A. Rodríguez, Generic dynamic scaling in kinetic roughening. Phys. Rev. Let. **84**, 2199 (2000)
19. M. Pelliccione, T.M. Lu, *Evolution of Thin Film Morphology: Modeling and Simulations*, 1st edn. (Springer, New York, 2008)
20. M. Pelliccione, T.-M. Lu, *Evolution of thin film morphology* (Springer, New York, 2008)
21. G. Pradhan, P.P. Dey, A.K. Sharma, Anomalous kinetic roughening in growth of MoS 2 films under pulsed laser deposition. RSC Adv. **9**, 12895 (2019)
22. F. Ruffino, M. Grimaldi, Atomic force microscopy study of the growth mechanisms of nanostructured sputtered Au film on Si (111): evolution with film thickness and annealing time. J. Appl. Phys. **107**, 104321 (2010)
23. M. Raible, S. Mayr, S.J. Linz, M. Moske, P. Hänggi, K. Samwer, Amorphous thin-film growth: theory compared with experiment. EPL Europhys. Lett. **50**, 61 (2000)
24. M. Kardar, G. Parisi, Y.-C. Zhang, Dynamic scaling of growing interfaces. Phys. Rev. Lett. **56**, 889 (1986)
25. W.W. Mullins, Theory of thermal grooving. J. Appl. Phys. **28**, 333 (1957)
26. S.F. Edwards, D. Wilkinson, The surface statistics of a granular aggregate. Proc. R. Soc. Lond. A Math. Phys. Sci. **381**, 17 (1982)
27. N. Tripathi, S. Rath, V. Ganesan, R. Choudhary, Growth dynamics of pulsed laser deposited indium oxide thin films: a substrate dependent study. Appl. Surf. Sci. **256**, 7091 (2010)
28. R. Dolbec, E. Irissou, M. Chaker, D. Guay, F. Rosei, M. El Khakani, Growth dynamics of pulsed laser deposited Pt nanoparticles on highly oriented pyrolitic graphite substrates. Phys. Rev. B **70**, 201406 (2004)
29. M.A. Auger, L. Vázquez, O. Sánchez, M. Jergel, R. Cuerno, M. Castro, Growth dynamics of reactive-sputtering-deposited AlN films. J. Appl. Phys. **97**, 123528 (2005)
30. I. Weaver, C. Lewis, Polar distribution of ablated atomic material during the pulsed laser deposition of Cu in vacuum: dependence on focused laser spot size and power density. J. Appl. Phys. **79**, 7216 (1996)
31. J.T. Drotar, Y.-P. Zhao, T.-M. Lu, G.-C. Wang, Surface roughening in shadowing growth and etching in $2+1$ dimensions. Phys. Rev. B **62**, 2118 (2000)
32. M. Grajower, U. Levy, J.B. Khurgin, The role of surface roughness in plasmonic-assisted internal photoemission schottky photodetectors. ACS Photon. **5**, 4030 (2018)
33. Kushwaha A, Aslam M, Roughness enhanced surface defects and photoconductivity of acid etched ZnO nanowires, in: *2012 International Conference on Emerging Electronics*, IEEE, pp. 1–4 (2012)
34. I. Herraiz-Cardona, E. Ortega, J.G. Antón, V. Pérez-Herranz, Assessment of the roughness factor effect and the intrinsic catalytic activity for hydrogen evolution reaction on Ni-based electrodeposits. Int. J. Hydrog. Energy **36**, 9428 (2011)
35. A.-K. Chan, H. Wang, M.J. Chan, High quality thermal oxide on LPSOI formed by high temperature enhanced MILC. IEEE Electron Device Lett. **22**, 384 (2001)